Orbital control of Rashba spin orbit coupling in noble metal surfaces

Shi-Jing Gong, Jia Cai, Qun-Fang Yao, Wen-Yi Tong, Xiangang Wan, Chun-Gang Duan, and J. H. Chu

Articles you may be interested in

Orbital dependent Rashba splitting and electron-phonon coupling of 2D Bi phase on Cu(100) surface
J. Chem. Phys. **139**, 184707 (2013); 10.1063/1.4828865

Spin and orbital magnetism of coinage metal trimers (Cu3, Ag3, Au3): A relativistic density functional theory study
AIP Advances **3**, 112122 (2013); 10.1063/1.4834336

Controlling the electrical transport properties of graphene by in situ metal deposition
Appl. Phys. Lett. **97**, 053107 (2010); 10.1063/1.3471396

Direct evidence of spin-polarized band structure of Sb(111) surface
Appl. Phys. Lett. **93**, 252107 (2008); 10.1063/1.3049610

Vibrational lifetimes of cyanide and carbon monoxide on noble and transition metal surfaces
J. Chem. Phys. **127**, 154303 (2007); 10.1063/1.2794744

Orbital control of Rashba spin orbit coupling in noble metal surfaces

Shi-Jing Gong,[1] Jia Cai,[1] Qun-Fang Yao,[1] Wen-Yi Tong,[1] Xiangang Wan,[2] Chun-Gang Duan,[1,a)] and J. H. Chu[1]

[1]*Key Laboratory of Polar Materials and Devices, Ministry of Education, East China Normal University, Shanghai 200062, China*
[2]*Department of Physics and National Laboratory of Solid State Microstructures, Nanjing University, Nanjing 210093, China*

Rashba spin orbit coupling (SOC) in noble metal surfaces is of great importance for the application of metal films in spintronic devices. By combining the density-functional theory calculations with our recently developed orbital selective external potential method, we investigate the Rashba SOC in the Shockley surface states of Au(111) and Ag(111). We find that the large Rashba SOC in the *sp*-character surface states of Au(111) is mainly contributed by the minor *d*-orbitals in the surface states. While for the *sd*-character surface states, although they are dominated by the *d*-orbitals, Rashba splitting is found to be rather small. Band structure analysis reveals that this is mainly because the *sd*-character surface states are well below the Fermi level and can be less influenced by the asymmetric surface potential. We demonstrate that the Rashba SOC in noble metal surfaces can be effectively manipulated by shifting the *d*-orbitals in the surface states, which can be physically implemented through surface decoration. Our investigation provides a deep understanding on Rashba SOC in noble metal surfaces and could be helpful to their applications in spintronic devices. © 2016 AIP Publishing LLC. [http://dx.doi.org/10.1063/1.4945320]

I. INTRODUCTION

The breaking of inversion symmetry in the surface of solid or interface of heterostructure could result in many spin-related phenomena, for example, the spontaneous spin splitting without magnetic field (usually called Rashba effect),[1,2] the topological surface states,[3,4] and the surface magnetic anisotropy of ferromagnetic metal films.[5,6] In fact, most of the spin-related phenomena at the surface/interface are related to the spin-orbit coupling (SOC),[7,8] which acts as a bridge between spin, orbital, and charge degrees of freedom. Among various kinds of SOCs, Rashba-type SOC[1] attracts growing research attention in both theoretical and experimental aspects,[9–19] because its strength can be flexibly tuned through electric field,[20–25] which *makes* it possible to electrically *manipulate* electron *spins*. Semiconductor heterostructure with Rashba SOC opens up the possibility to design all-electric devices,[26–28] for example, the well-known Datta-Das spin field transistor,[28] in which the spin precession can be controlled without the requirement of magnetic field.

Subsequent to the semiconductors,[29–34] metal surfaces become another important system with sizable Rashba SOC.[35–45] Research interest in metal surfaces begins with Au(111).[43] In 1996, LaShell *et al.* observed the SOC induced spin splitting in Au(111) surface by angle-resolved photoemission spectroscopy (ARPES).[43] At the Fermi wavevector, the splitting energy can reach up to 110 meV.[43] In 2001, Nicolay *et al.* reexamined Au(111) and Ag(111) surfaces by the high-resolution photoemission and fully relativistic calculations.[44] They observed a large spin splitting in Au(111) surface; however, they found the spin splitting in Ag(111) is

too small to be experimentally resolved. They attributed the large difference between Au(111) and Ag(111) to the different atomic SOC, as well as the potential gradient at the surface. In 2003, Henk *et al.* demonstrated that the spin polarization in the surface states of Au(111) is perpendicular to the in-plane wavevector, which can be well described by the Rashba SOC model.[45] Because the splitting bands in Au(111) surface are around the Fermi level and mainly consist of *s*- and *p*-orbitals, they are also called the shallow *sp*-character surface states,[46] and less attention has been paid to the minor *d*-orbitals hybridized in the surface states. Till in 2006, Bihlmayer *et al.* pointed out that a surface state of purely *p*- or *d*-orbitals shows no Rashba splitting at all, only the hybridization of different-parity orbitals in the surface state wave functions can result in the asymmetry of the wavefunction and induce Rashba SOC.[47] This is the first time that the contribution of the *d*-orbitals is pointed out. More recently in 2012, Lee and Choi studied Au(111) and Ag(111) surfaces and reported the exciting finding that the *d*-orbitals determine the Rashba splitting.[49] The proximity of 5*d*- and 6*s*-orbital energy levels in Au increases the *d*-orbitals in the surface states,[48] which may be the genuine reason why Rashba splitting in Au(111) is much larger than that in Ag(111). In addition, Nagano *et al.* investigated the Rashba SOC in different Au crystalline surfaces and found that the Rashba SOC in Au(110) is much different from that in Au(111), because the surface states of the outmost surface layer of Au(110) and Au(111) are composed mostly of the surface-parallel and surface-normal *p*-orbitals, respectively.[48]

Meanwhile, various approaches have been tried to tune the Rashba SOC strength in metal surfaces.[50–55] Ast *et al.* designed the surface alloy Bi/Ag(111), in which a giant Rashba spin splitting is obtained due to the coexistence of

a)Electronic mail: cgduan@clpm.ecnu.edu.cn

strong in-plane and out-of-plane potential gradient.[51] Mirhosseini and Abdelouahed *et al*. constructed the metal/ferroelectric (Bi/BaTiO$_3$) interface, in which they found the reversal of the ferroelectric polarization can change the Rashba splitting.[54,55] In our previous work, we found that the directly applying electric field can tune the Rashba SOC in Au(111) surface.[51] However, due to the screening effect at the metal surface, the impact of the electric field is relatively limited. In the present work, by combining the density-functional theory (DFT) calculations with our recently developed orbital selective external potential (OSEP) method,[56,57] we comparatively investigate the *sp*- and *sd*-character surface states[58] in noble metal surfaces Au(111) and Ag(111, and reveal the orbital dependence of Rashba SOC. Guided by the orbital analysis, we can intentionally tailor the orbital components in the surface states through surface decoration, whereby we can effectively control the strength of Rashba SOC.

II. COMPUTATIONAL METHODS

The calculations are performed within relativistic DFT using the projector augmented wave (PAW) method implemented in the Vienna *Ab-Initio* Simulation Package (VASP).[59] The exchange-correlation potential is treated in the local-spin-density approximation (LSDA), with SOC included. We use the energy cut-off of 400 eV for the plane wave expansion of the PAWs and a $21 \times 21 \times 1$ Γ centered *k*-point grid in the self-consistent calculations. For geometry optimization, all the internal coordinates are relaxed until the
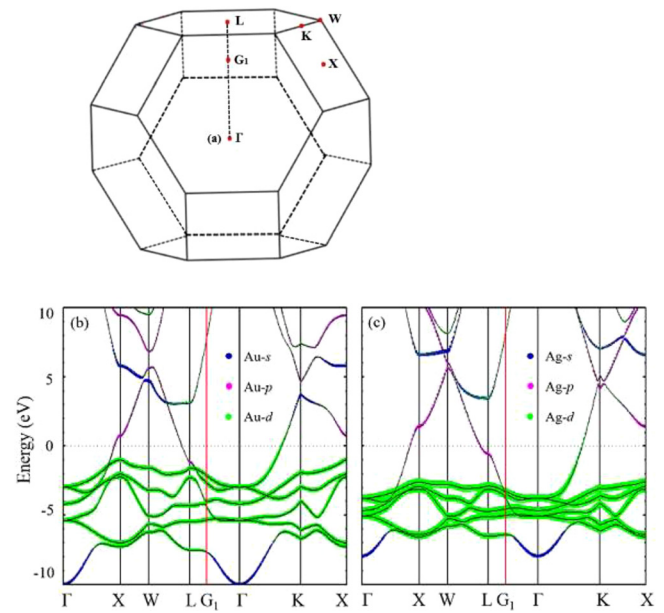

FIG. 1. (a) The first Brillouin zone of a face-centered-cubic crystal, in which Γ, X, W, L, and K are the high symmetry k-points. The orbital-projected band structures of bulk (b) Au and (c) Ag, with the blue, pink, and green dots indicating the *s*-, *p*-, and *d*-orbital states, respectively. The radii of circles are proportional to the weight of the corresponding orbital. The Fermi level is set to be zero.

Hellmann-Feynman forces are less than 1 meV/Å. The vacuum thickness along the *z* axis is 20 Å, which is thick enough to avoid the interaction between adjacent slabs.
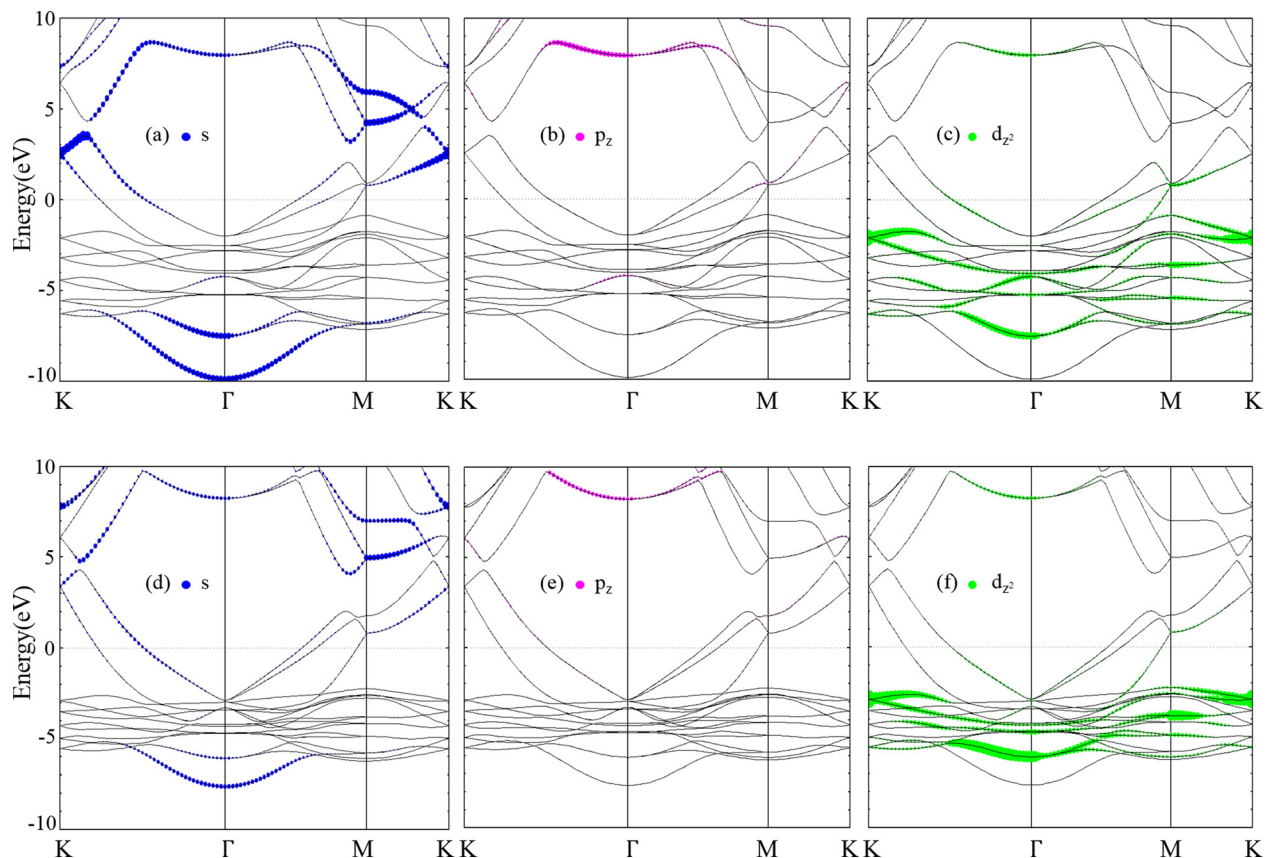

FIG. 2. Orbital-projected band structures of bulk (a)–(c) Au and (d)–(f) Ag for hexagonal close-packed unit cell, with the blue, pink, and green dots indicating the *s*, p_z, and d_z^2 orbitals, respectively.

We use the OSEP method[56,57] to investigate the orbital-dependence of Rashba SOC in noble metal surfaces. This method can introduce a special external potential on the selected orbitals, which has some similarity with the DFT $+ U$ method. Within the frame of OSEP, the system Hamiltonian is written as $H^{OSEP} = H_{KS}^0 + |inlm\sigma\rangle\langle inlm\sigma|V_{ext}$, where H_{KS}^0 is the primary Kohn–Sham Hamiltonian, and V_{ext} is the applied potential energy. The indices i, n, l, m, and σ represent the atom site, principle, orbital, magnetic, and spin quantum number, respectively. Since the strength of hybridization between two orbitals is strongly dependent on their energy difference, we therefore can control the hybridization by applying an external field to shift the energy levels of the orbitals. Here, we use this method to control the orbital hybridization in the surface states and demonstrate the contributions of the different orbitals to Rashba SOC.

III. RESULTS AND DISCUSSION

A. Band structures of bulk Au and Ag for primitive unit cell

Noble metals Au $(5d^{10}6s^1)$ and Ag $(4d^{10}5s^1)$ have the same face centered cubic (FCC) structure, with the primitive unit cell including a single atom. Fig. 1(a) shows the first

Brillouin zone (BZ) of a FCC lattice, with the high symmetry k-points Γ, X, W, L, and K. In Figs. 1(b) and 1(c), the orbital-projected band structures of bulk Au and Ag are shown, respectively, with the blue, pink, and green dots indicating the s-, p-, and d-orbital states, respectively. For both Au and Ag, we can find the occupied s orbital below the Fermi level, which shows a characteristic free-electron-like behavior around the Γ point. We also notice the empty s orbital above the Fermi level, because Au (Ag) atom has only one $6s$ $(5s)$ electron. In addition, we can clearly see the nearly fully filled d orbitals below the Fermi level and the empty p orbitals above the Fermi level.

B. Band structures of bulk Au and Ag for the hexagonal close-packed (HCP) unit cell

The (111) surface is obtained by cutting the FCC structure in the way that the surface plane intersects the x-, y-, and z- axes at the same value, which exposes a surface with hexagonal arrangement. The HCP unit cell has three times the volume of the primitive unit cell, and the three k-points in the first BZ, i.e., $\Gamma(0, 0, 0)$, G1$(1/3, 1/3, 1/3)$, and G1$'(-1/3, -1/3, -1/3)$ shown in Fig. 1(a), coincide at the Γ point in the BZ of the hexagonal unit cell. In Figs. 2(a)–2(f), the orbital-projected band structures of bulk Au and Ag for HCP unit
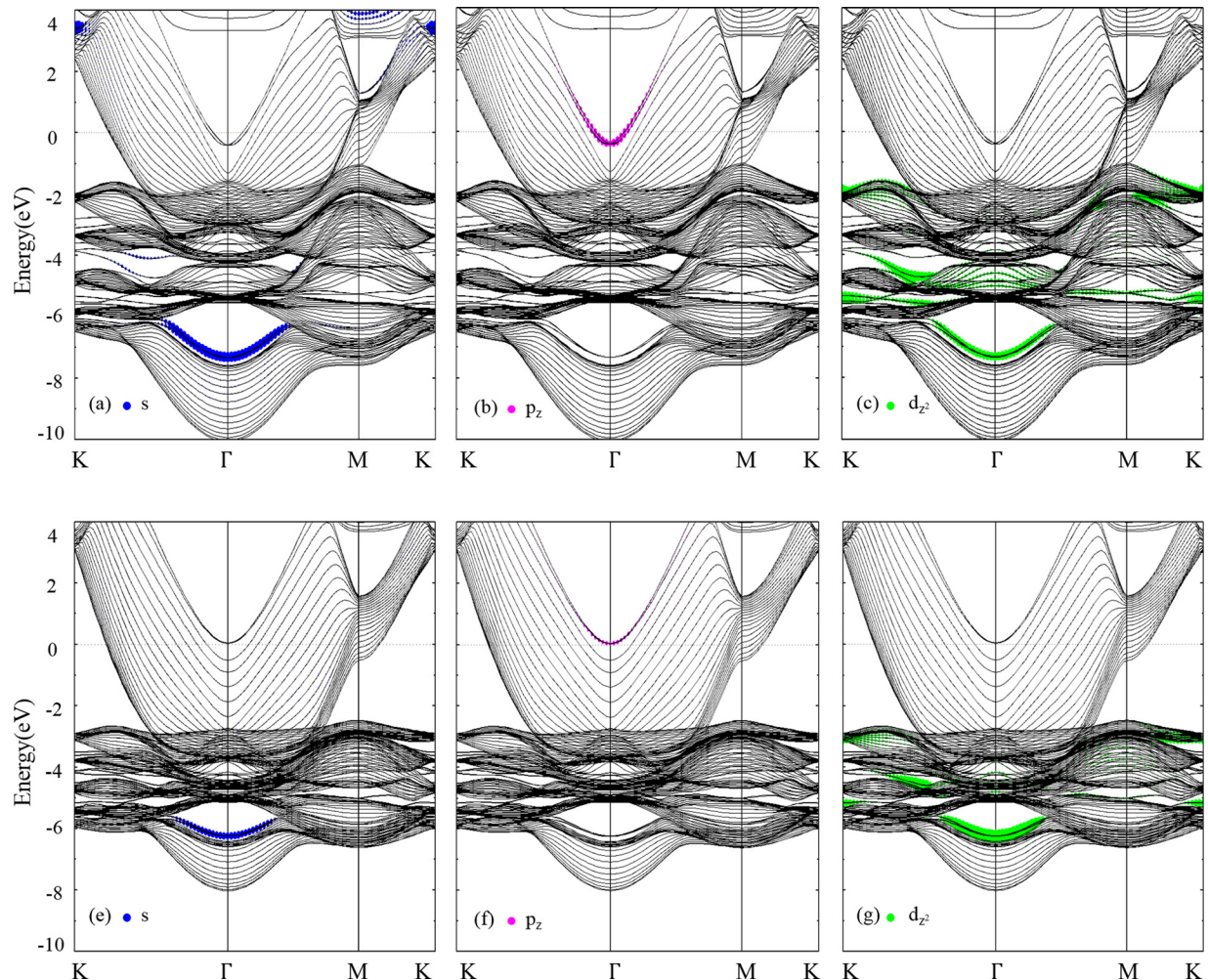

FIG. 3. Orbital-projected band structures of (a)–(c) Au(111) and (d)–(f) Ag(111) slabs, with the blue, pink, and green colors representing the s, p_z, and $d_z{}^2$ orbitals of the surface Au (Ag) atom, respectively.

cell are shown, in which the blue, pink, and green dots indicate the s, p_z, and d_{z^2} orbital states, respectively. We specially present the p_z and d_{z^2} orbitals, because these z-oriented orbitals are sensitive to the surface potential and play the critical role in forming Rashba SOC. Both in Au(111) and Ag(111) surfaces, we can observe the bands around 8 eV above the Fermi level, which consist of s, p_z, and d_{z^2} orbitals. In addition, we also notice the bands around 6 eV below the Fermi level, which are mainly contributed by s and d_{z^2} orbitals. To simplify the description, we name the bands around 8 eV and −6 eV as S1 and S2, respectively. Bands S1 and S2 will evolve into the shallow sp- and deep sd-character surface states, which will be discussed in the following.

C. Rashba spin orbit coupling in Au(111) and Ag(111) surfaces

We then investigate the surface states of Au(111) and Ag(111). In Fig. 3, we plot the orbital-projected band structures of the 22-layer Au(111) and Ag(111) slabs, in which the blue, pink, and green colors represent the s, p_z, and d_{z^2} orbitals of the surface Au (Ag) atom in the slab, respectively. Both in Au(111) and Ag(111), we can clearly observe the surface states around the Fermi level, i.e., the well-known sp-character surface states. Also, we can clearly see the deep sd-character surface states, which are located well below the Fermi level. From the orbital analysis, we know that the shallow sp-character surface states are dominated by the p_z orbital, and the deep sd-character surface states mainly consist of the s and d_{z^2} orbitals.

Compare band structures of Au(111) bulk and its slab, we notice that Au S1 bands are around 8 eV, and the sp-character Rashba splitting bands are around the Fermi level. Yet the energy levels of Au S2 bands and the sd-character bands do not show much difference, which means that the sd-character surface states are less influenced by the surface potential. To clearly show the sp- and sd-character surface states, we select different energy windows in Figs. 4(a) and 4(b), in which we can see that the Rashba splitting of the sp-character surface states is much larger than that of the sd-character ones. Similar comparison is also conducted between Ag(111) bulk and its slab. A large energy difference between Ag S1 bands and the sp-character splitting bands is also observed; however, the surface potential gradient does not induce the large Rashba SOC in Ag(111) surface.

D. Orbital dependence of Rashba spin orbit coupling

Using our recently developed OSEP method, we can artificially control the orbital components in the surface states, and therefore reveal their contributions to Rashba SOC. Due to the orbital angular momentum $l = 0$, the s-orbital is believed to have no contribution to Rashba SOC. To distinguish the contributions of the p- and d-orbitals, we consider an external field selectively applied to the d-orbitals by using the OSEP method. In Figs. 4(c) and 4(d), we show the band structures of Au(111) slab with $V_{ext}^d = -3$ eV. We notice that the sd-character surface states are shifted down, with Rashba splitting greatly enhanced. While the sp-character splitting bands are pushed upward, and the Rashba splitting is obviously suppressed. Because the total number of
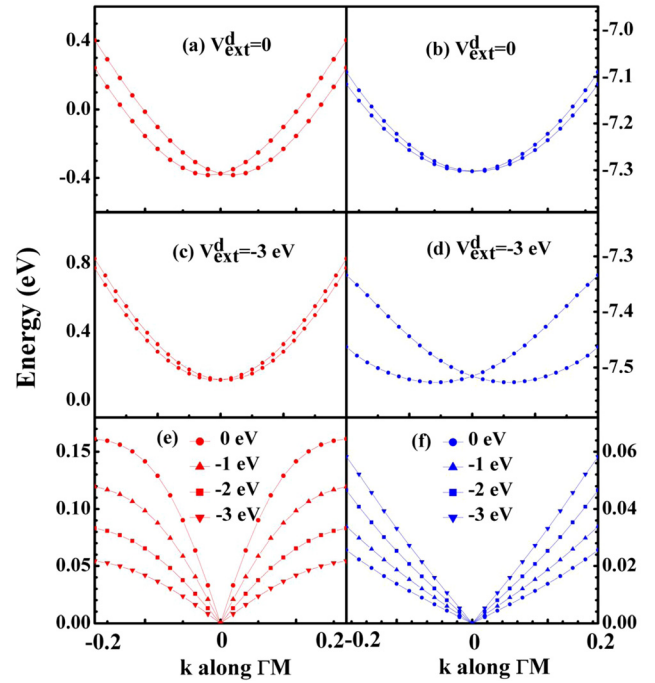

FIG. 4. The sp- and sd- character Rashba spin splitting bands in Au(111) with (a), (b) $V_{ext}^d = 0$ and (c), (d) $V_{ext}^d = -3$ eV. Rashba splitting energy of the (e) sp- and (f) sd-character surface states under different values of d-orbital potential energy $V_{ext}^d = 0, -1, -2, -3$ eV.
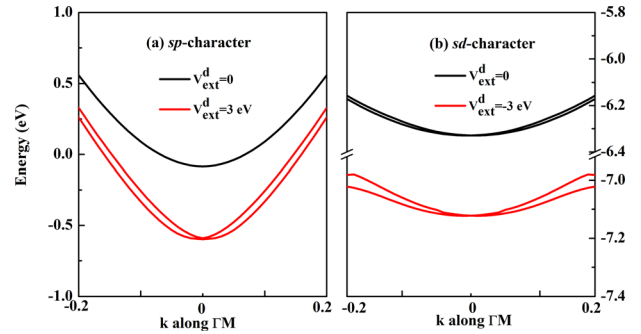

FIG. 5. Rashba spin splitting bands in Ag(111), (a) the sp-character splitting bands with $V_{ext}^d = 0$ and 3 eV, and (b) the sd-character splitting bands with $V_{ext}^d = 0$ and −3 eV.
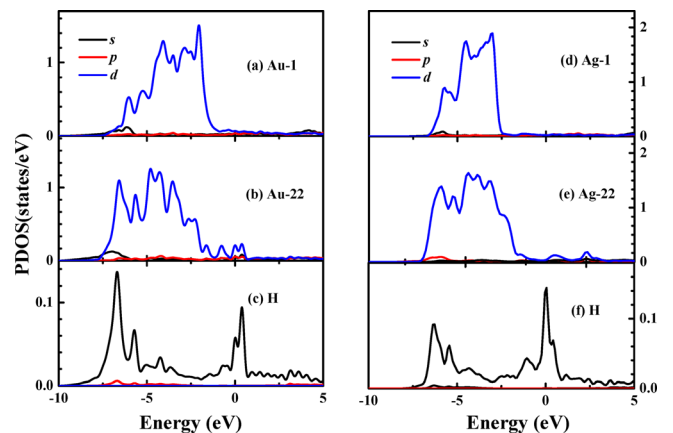

FIG. 6. The partial density of states of (a) Au-1, (b) Au-22, and (c) H in H/Au(111) system. Similarly, figures (d)–(f) correspond to Ag-1, Ag-22, and H in H/Ag(111) system.

electrons is constant, the fact that more *d*-orbitals are occupied due to the shifting down of the *d*-orbitals will consequently result in less occupation of *s*- or *p*-orbitals. This is the reason why the *sp*-character surface states are shifted upward and thus become empty. In Figs. 4(e) and 4(f), the Rashba splitting energy under different values of *d*-orbital potential energy is presented. It is obvious that the Rashba splitting energies of the *sp*- and *sd*-character surface states show opposite behaviors, and both are closely dependent on the *d*-orbital potential energy. We also notice the nonlinear relationship between the Rashba splitting energy and the wavevector, which has been discussed previously.[29,39,52]

Similar calculations are also conducted for Ag(111) surface. To enhance Rashba SOC strength of the *sp*- and *sd*-character surface states in Ag(111) surface, we should apply different *d*-orbital fields. In Fig. 5(a), we show the Rashba spin splitting of the *sp*-character surface states, with the red curves representing $V_{ext}^d = 3$ eV. In Fig. 5(b), we show the Rashba spin splitting of the *sd*-character surface states, with the red curves representing $V_{ext}^d = -3$ eV. The black curves in Figs. 5(a) and 5(b) represent $V_{ext}^d = 0$, which are provided for comparison. We find that the positive *d*-orbital potential energy can increase the Rashba splitting of the *sp*-character surface states, while the negative *d*-orbital potential energy can increase the Rashba splitting of the *sd*-character surface states.

E. Surface decoration

From the above calculations based on OSEP method, we confirm that the Rashba SOC in both Au(111) and Ag(111)

is sensitive to the *d*-orbitals in their surface states. How can we physically modify the *d*-orbitals distribution? It was reported by Sakong and Groß that the hydrogen adsorption on Cu(111) surface can shift down the *d*-orbitals of surface copper atom.[60] They found the top site adsorption, with the hydrogen atom mainly interacting with one copper atom, can induce the obvious shifting down of the *d*-bands, due to the strong hybridization between H *1s* and Cu $3d_{z^2}$.[60] Since Au, Ag, and Cu are in the same column in the element periodic table, they may have similar properties, based on which we presently investigate the influence of hydrogen adsorption on the surface states of Au(111) and Ag(111).

We consider the model that one surface of the noble metal slab is adsorbed by hydrogen atom, with one hydrogen adatom per unit cell, and the other surface remains clean. For both H/Au(111) and H/Ag(111), we notice that the top site *adsorption* is not *energetically favorable*, yet it can induce the obvious shifting down of the *d*-orbitals, which is similar with the case of H/Cu(111). For top site adsorption, we present partial density of states (PDOS) of the hydrogen adatom and the surface Au atoms in Figs. 6(a)–6(c). To simplify the description, the Au atom on the clean Au(111) surface is labeled as Au-1, and the Au atom on the adsorbed surface, which directly contacts with hydrogen atom, is Au-22. Comparing PDOS of Au-1 and Au-22, we find that the adsorption of hydrogen atom pushes down the *d*-orbitals of Au-22. An obvious hybridization between H *1s* orbital and Au-22 *5d* orbitals can be inferred from Figs. 6(b) and 6(c). The orbital projected band structures will further demonstrate the hybridization between H *1s* and Au-22 $5d_{z^2}$, which will be discussed in the following.
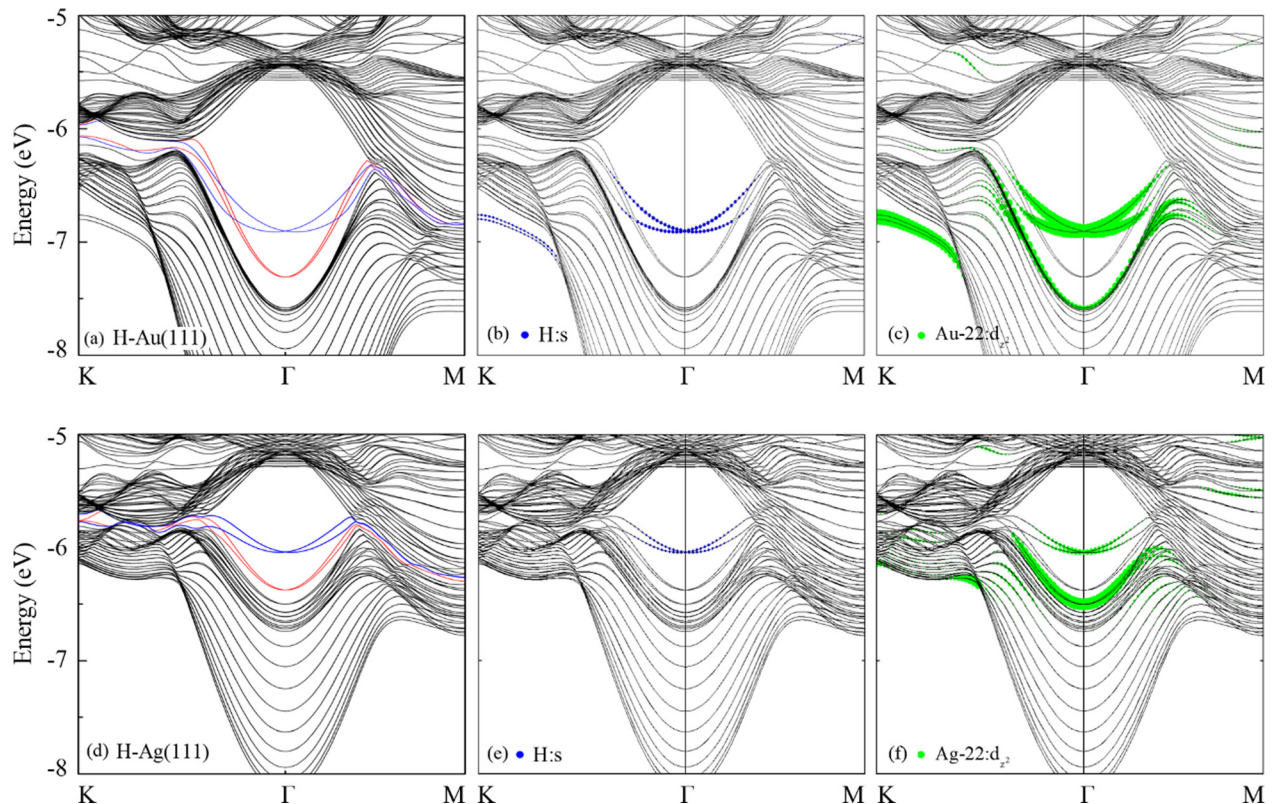

FIG. 7. Band structures of (a) H/Au(111) and (d) H/Ag(111), in which the red and blue curves indicate the *sd*-character splitting bands of the clean and adsorbed surfaces, respectively. The orbital-projected band structures of (b), (c) H/Au(111) and (e), (f) H/Ag(111), with H 1s shown in blue and Au (Ag) d_z^2 in green.

The results of H/Ag(111) system are shown in Figs. 6(d)–6(f), and similar effects can also be observed.

To observe the influence of *d*-orbitals shifting on Rashba SOC, we plot the band structures of the H/Au(111) and H/Ag(111) in Figs. 7(a) and 7(d), respectively, in which the blue curves indicate the *sd*-character surface states of the adsorbed surface, and the red ones represent the clean surface. Both in H/Ag(111) and H/Au(111), we find the *sd*-character Rashba splitting is greatly enhanced by hydrogen adsorption. Even Rashba splitting in H/Ag(111) is comparable to that in H/Au(111). We then show the orbital-projected band structures of H/Au(111) in Figs. 7(b) and 7(c), and H/Ag(111) in Figs. 7(e) and 7(f), in which the H 1*s* orbital is shown in blue, and the d_{z^2} orbital of the surface Au (Ag) atom is in green. It can be clearly seen that the *sd*-character splitting bands of the adsorbed surface mainly consist of the H 1*s* orbital and d_{z^2} orbital of the surface Au (Ag) atom. We believe that it is the hybridization between H 1*s* and Au $5d_{z^2}$ (Ag $4d_{z^2}$) that shifts down the *d*-orbital bands and enhances the Rashba SOC.

IV. SUMMARY

In summary, we investigate the Rashba SOC in Au(111) and Ag(111) surfaces. We confirm that the Rashba SOC in the *sp*-character surface states of Au(111) is much larger than that of Ag(111), and the minor *d*-orbitals in the surface states play the critical role in forming large Rashba SOC. Although the *sd*-character surface states in both Au(111) and Ag(111) surfaces are dominated by the *d*-orbitals, the Rashba splitting in them is found to be rather small. Band structure analysis reveals that this is mainly because these *sd*-character surface states are well below the Fermi level and can be less influenced by the asymmetric surface potential. Using the orbital selective external potential method, we find that the Rashba splitting in both the *sp*- and *sd*-character surface states can be effectively manipulated by shifting the *d*-orbitals in the surface states. Furthermore, we find such *d*-orbital potential energy can be physically implemented through surface decoration. For example, the adsorption of hydrogen atom can obviously shift down the *d*-orbitals in the surface states and greatly enhance the Rashba SOC in the *sd*-character surface states of both Au(111) and Ag(111). Our investigation provides a deep understanding on Rashba SOC in noble metal surfaces and would be helpful to their applications in spintronic devices.

ACKNOWLEDGMENTS

[1]Y. A. Bychkov and E. I. Rashba, J. Phys. C: Solid State Phys. **17**, 6039 (1984).
[2]A. Manchon, H. C. Koo, J. Nitta, S. M. Frolov, and R. A. Duine, Nat. Mater. **14**, 871 (2015).
[3]M. Z. Hasan and C. L. Kane, Rev. Mod. Phys. **82**, 3045 (2010).
[4]C. L. Kane and E. J. Mele, Phys. Rev. Lett. **95**, 226801 (2005).
[5]M. Weisheit, S. Fähler, A. Marty, Y. Souche, C. Poinsignon, and D. Givord, Science **315**, 349 (2007).
[6]C.-G. Duan, J. P. Velev, R. F. Sabirianov, Z. Zhu, J. Chu, S. S. Jaswal, and E. Y. Tsymbal, Phys. Rev. Lett. **101**, 137201 (2008).
[7]R. Winkler, *Spin-Orbit Coupling Effects in Two-Dimensional Electron and Hole Systems* (Springer, Berlin; New York, 2003).
[8]G. Dresselhaus, Phys. Rev. **100**, 580 (1955).
[9]S. J. Gong, Z. Y. Li, Z. Q. Yang, C. Gong, C. G. Duan, and J. H. Chu, J. Appl. Phys. **110**, 043704 (2011).
[10]O. Rader, A. Varykhalov, J. Sánchez-Barriga, D. Marchenko, A. Rybkin, and A. M. Shikin, Phys. Rev. Lett. **102**, 057602 (2009).
[11]Y. S. Dedkov, M. Fonin, U. Rüdiger, and C. Laubschat, Phys. Rev. Lett. **100**, 107602 (2008).
[12]A. Varykhalov, D. Marchenko, M. R. Scholz, E. D. L. Rienks, T. K. Kim, G. Bihlmayer, J. Sánchez-Barriga, and O. Rader, Phys. Rev. Lett. **108**, 066804 (2012).
[13]K. Ishizaka *et al.*, Nat. Mater. **10**, 521 (2011).
[14]T. G. A. Verhagen, I. Leermakers, J. M. van Ruitenbeek, and J. Aarts, Phys. Rev. B **91**, 184402 (2015).
[15]L. Meier, G. Salis, I. Shorubalko, E. Gini, S. Schon, and K. Ensslin, Nat. Phys. **3**, 650 (2007).
[16]G. Herranz *et al.*, Nat. Commun. **6**, 6028 (2015).
[17]S. R. Park, C. H. Kim, J. Yu, J. H. Han, and C. Kim, Phys. Rev. Lett. **107**, 156803 (2011).
[18]K. Yaji, Y. Ohtsubo, S. Hatta, H. Okuyama, K. Miyamoto, T. Okuda, A. Kimura, H. Namatame, M. Taniguchi, and T. Aruga, Nat. Commun. **1**, 17 (2010).
[19]I. M. Miron, G. Gaudin, S. Auffret, B. Rodmacq, A. Schuhl, S. Pizzini, J. Vogel, and P. Gambardella, Nat. Mater. **9**, 230 (2010).
[20]J. Nitta and T. Bergsten, IEEE Trans. Electron Devices **54**, 955 (2007).
[21]Y. H. Park, S.-H. Shin, J. D. Song, J. Chang, S. H. Han, H.-J. Choi, and H. C. Koo, Solid State Electron. **82**, 34 (2013).
[22]D. Liang and X. P. A. Gao, Nano Lett. **12**, 3263 (2012).
[23]S. E. Barnes, J. I. Ieda, and S. Maekawa, Sci. Rep. **4**, 4105 (2014).
[24]L. Xu and S. Zhang, J. Appl. Phys. **111**, 07C501 (2012).
[25]J. Nitta, T. Bergsten, Y. Kunihashi, and M. Kohda, J. Appl. Phys. **105**, 122402 (2009).
[26]S.-J. Gong, H.-C. Ding, W.-J. Zhu, C.-G. Duan, Z. Zhu, and J. Chu, Sci. China: Phys., Mech. Astron. **56**, 232 (2013).
[27]S. J. Gong and Z. Q. Yang, Phys. Lett. A **367**, 369 (2007).
[28]S. Datta and B. Das, Appl. Phys. Lett. **56**, 665 (1990).
[29]W. Yang and K. Chang, Phys. Rev. B **74**, 193314 (2006).
[30]D. Culcer and R. Winkler, Phys. Rev. B **76**, 245322 (2007).
[31]D. Culcer and R. Winkler, Phys. Rev. Lett. **99**, 226601 (2007).
[32]R. Winkler, Phys. Rev. B **69**, 045317 (2004).
[33]D. Culcer, Y. Yao, A. H. MacDonald, and Q. Niu, Phys. Rev. B **72**, 045215 (2005).
[34]J. Sinova, D. Culcer, Q. Niu, N. A. Sinitsyn, T. Jungwirth, and A. H. MacDonald, Phys. Rev. Lett. **92**, 126603 (2004).
[35]A. Bendounan, K. Aït-Mansour, J. Braun, J. Minár, S. Bornemann, R. Fasel, O. Gröning, F. Sirotti, and H. Ebert, Phys. Rev. B **83**, 195427 (2011).
[36]Y. M. Koroteev, G. Bihlmayer, J. E. Gayone, E. V. Chulkov, S. Blügel, P. M. Echenique, and P. Hofmann, Phys. Rev. Lett. **93**, 046403 (2004).
[37]A. M. Shikin, A. A. Rybkina, M. V. Rusinova, I. I. Klimovskikh, A. G. Rybkin, E. V. Zhizhin, E. V. Chulkov, and E. E. Krasovskii, New J. Phys. **15**, 125014 (2013).
[38]O. Krupin, G. Bihlmayer, K. M. Döbrich, J. E. Prieto, K. Starke, S. Gorovikov, S. Blügel, S. Kevan, and G. Kaindl, New J. Phys. **11**, 013035 (2009).
[39]H. Ishida, Phys. Rev. B **90**, 235422 (2014).
[40]S. N. P. Wissing, C. Eibl, A. Zumbülte, A. B. Schmidt, J. Braun, J. Minár, H. Ebert, and M. Donath, New J. Phys. **15**, 105001 (2013).
[41]D. Marchenko, A. Varykhalov, M. R. Scholz, G. Bihlmayer, E. I. Rashba, A. Rybkin, A. M. Shikin, and O. Rader, Nat. Commun. **3**, 1232 (2012).
[42]A. Tamai, W. Meevasana, P. D. C. King, C. W. Nicholson, A. de la Torre, E. Rozbicki, and F. Baumberger, Phys. Rev. B **87**, 075113 (2013).
[43]S. LaShell, B. A. McDougall, and E. Jensen, Phys. Rev. Lett. **77**, 3419 (1996).
[44]G. Nicolay, F. Reinert, S. Hüfner, and P. Blaha, Phys. Rev. B **65**, 033407 (2001).
[45]J. Henk, A. Ernst, and P. Bruno, Phys. Rev. B **68**, 165416 (2003).
[46]L. Petersen and P. Hedegård, Surf. Sci. **459**, 49 (2000).
[47]G. Bihlmayer, Y. M. Koroteev, P. M. Echenique, E. V. Chulkov, and S. Blügel, Surf. Sci. **600**, 3888 (2006).
[48]M. Nagano, A. Kodama, T. Shishidou, and T. Oguchi, J. Phys.: Condens. Matter **21**, 064239 (2009).

[49]H. Lee and H. J. Choi, Phys. Rev. B **86**, 045437 (2012).

[50]D. Di Sante, P. Barone, R. Bertacco, and S. Picozzi, Adv. Mater. **25**, 509 (2013).

[51]C. R. Ast, J. Henk, A. Ernst, L. Moreschini, M. C. Falub, D. Pacilé, P. Bruno, K. Kern, and M. Grioni, Phys. Rev. Lett. **98**, 186807 (2007).

[52]S.-J. Gong, C.-G. Duan, Y. Zhu, Z.-Q. Zhu, and J.-H. Chu, Phys. Rev. B **87**, 035403 (2013).

[53]Y. Zhang, T.-T. Tang, C. Girit, Z. Hao, M. C. Martin, A. Zettl, M. F. Crommie, Y. R. Shen, and F. Wang, Nature **459**, 820 (2009).

[54]S. Abdelouahed and J. Henk, Phys. Rev. B **82**, 193411 (2010).

[55]H. Mirhosseini, I. V. Maznichenko, S. Abdelouahed, S. Ostanin, A. Ernst, I. Mertig, and J. Henk, Phys. Rev. B **81**, 073406 (2010).

[56]X. G. Wan, J. Zhou, and J. M. Dong, Europhys. Lett. **92**, 57007 (2010).

[57]Y. Du, H.-C. Ding, L. Sheng, S. Y. Savrasov, X. Wan, and C.-G. Duan, J. Phys.: Condens. Matter **26**, 025503 (2014).

[58]R. Mazzarello, A. D. Corso, and E. Tosatti, Surf. Sci. **602**, 893 (2008).

[59]G. Kresse and D. Joubert, Phys. Rev. B **59**, 1758 (1999).

[60]S. Sakong and A. Groß, Surf. Sci. **525**, 107 (2003).